Mon. Not. R. Astron. Soc. **000**, 1–13 (2004) Printed 5 April 2005 (MN LATEX style file v2.2)

# Asteroseismology of the $\beta$ Cephei star $\nu$ Eridani – IV. The 2003-4 multisite photometric campaign and the combined 2002-4 data

M. Jerzykiewicz[1⋆], G. Handler[2], R. R. Shobbrook[3]†, A. Pigulski[1], R. Medupe[4,5], T. Mokgwetsi[4], P. Tlhagwane[4] and E. Rodríguez[6]
[1] *Wrocław University Observatory, ul. Kopernika 11, 51-622 Wrocław, Poland*
[2] *Institut für Astronomie, Universität Wien, Türkenschanzstrasse 17, A-1180 Wien, Austria*
[3] *Research School of Astronomy and Astrophysics, Australian National University, Canberra, ACT, Australia*
[4] *Theoretical Astrophysics Programme, North West University, Private Bag X2046, Mmabatho 2735, South Africa*
[5] *South African Astronomical Observatory, PO Box 9, Observatory 7935, South Africa*
[6] *Instituto de Astrofisica de Andalucia, C.S.I.C., Apdo. 3004, 18080 Granada, Spain*

Accepted 2005 April 6. Received 2005 April 6; in original form 2005 February 2

**ABSTRACT**
The second multisite photometric campaign devoted to $\nu$ Eri is reported. The campaign, carried out from 11 Sept. 2003 to 16 Feb. 2004, was very nearly a replica of the first, 2002-3 one: the five telescopes and photometers we used were the same as those in the first campaign, the comparison stars and observing procedure were identical, and the numbers and time base-lines of the data were comparable.

For $\nu$ Eri, analysis of the new data adds four independent frequencies to the nine derived previously from the 2002-3 data, three in the range from 7.20 to 7.93 $d^{-1}$, and a low one, equal to 0.614 $d^{-1}$. Combining the new and the old data results in two further independent frequencies, equal to 6.7322 and 6.2236 $d^{-1}$. Altogether, the oscillation spectrum is shown to consist of 12 high frequencies and two low ones. The latter have $u$ amplitudes about twice as large as the $v$ and $y$ amplitudes, a signature of high radial-order $g$ modes. Thus, the suggestion that $\nu$ Eri is both a $\beta$ Cephei and an SPB star, put forward on the basis of the first campaign's data, is confirmed.

Nine of the 12 high frequencies form three triplets, of which two are new. The triplets represent rotationally split $\ell = 1$ modes, although in case of the smallest-amplitude one this may be questioned. Mean separations and asymmetries of the triplets are derived with accuracy sufficient for meaningful comparison with models.

The first comparison star, $\mu$ Eri, is shown to be an SPB variable with an oscillation spectrum consisting of six frequencies, three of which are equidistant in period. The star is also found to be an eclipsing variable. The eclipse is a transit, probably total, the secondary is fainter than the primary by several magnitudes, and the system is widely detached.

The second comparison star, $\xi$ Eri, is confirmed to be a $\delta$ Scuti variable. To the frequency of 10.8742 $d^{-1}$ seen already in the first campaign's data, another one, equal to 17.2524 $d^{-1}$, is added.

**Key words:** techniques: photometric – stars: early-type – stars: individual: $\nu$ Eridani – stars: individual: $\mu$ Eridani – stars: individual: $\xi$ Eridani – stars: oscillations – stars: eclipsing

## 1 INTRODUCTION

The first multisite photometric and spectrographic campaign devoted to the $\beta$ Cephei star $\nu$ Eridani was carried out between October 2002 and February 2003. More than 600 h of differential $uvyV$ photometry on 148 nights and

⋆ E-mail: mjerz@astro.uni.wroc.pl
† Visiting Fellow

more than 2000 high-resolution spectra were obtained. A frequency analysis of the photometric data was reported by Handler et al. (2004, hereafter Paper I), while the spectrographic time-series and their analysis were presented by Aerts et al. (2004, hereafter Paper II). An extended frequency analysis and mode identification was provided by De Ridder et al. (2004, hereafter Paper III).

Seismic modelling of the oscillation spectrum of $\nu$ Eri has been undertaken by Pamyatnykh, Handler & Dziembowski (2004) and Ausseloos et al. (2004).

In Paper I, the light-variation of $\nu$ Eri was shown to consist of 23 sinusoidal terms. These included 8 independent ones with frequencies, $f_i$, $i = 1..8$, spanning the range from 5.6 to 7.9 $d^{-1}$, 14 high-frequency combination terms, and a term with the low frequency $f_A = 0.432$ $d^{-1}$.

The four highest-amplitude terms, discovered long ago by Saito (1976), consist of a singlet with frequency $f_1 = 5.763$ $d^{-1}$, and a triplet very nearly equidistant in frequency ($f_3 = 5.620$, $f_4 = 5.637$ and $f_2 = 5.654$ $d^{-1}$). Before the campaign it was known that the singlet was a radial mode (Cugier, Dziembowski & Pamyatnykh 1994), and surmised that it was the fundamental (Dziembowski & Jerzykiewicz 2003), but the true nature of the triplet was unclear. From multicolour photometry, Heynderickx, Waelkens & Smeyers (1994) derived $\ell = 1$ for $f_4$, and suggested that the triplet was a rotationally split dipole mode. This was challenged by Aerts, Waelkens & de Pauw (1994) who—from an analysis of line-profile variations—identified the $f_2$ term with an axisymmetric mode. However, both results are questionable because in neither case the triplet had been resolved. The matter was settled in Paper III: the wavelength dependence of the *uvy* amplitudes of the triplet terms implies $\ell = 1$ for all of them. Pamyatnykh et al. (2004) showed then that the triplet was a $g_1$ mode.

A frequency triplet $f_- < f_0 < f_+$ can be characterized by its mean separation

$$S = 0.5(f_+ - f_-), \tag{1}$$

and asymmetry

$$A = f_- + f_+ - 2f_0. \tag{2}$$

In case of a rotationally split triplet, $S$ is determined by the angular rotation rate of the star, $\Omega$, while $A$ is sensitive to effects of higher order in $\Omega$, as well as to effects of a magnetic field. If these effects are negligible, $A = 0$.

For the $i = 3, 4, 2$ triplet, both parameters were derived before the campaign from archival data by Dziembowski & Jerzykiewicz (2003). The value of asymmetry they obtained, $A = (-7.1 \pm 0.3) \times 10^{-4}$ $d^{-1}$, was unexpectedly large for the small rotation rate implied by the triplet's $S = 0.0168$ $d^{-1}$. Dziembowski & Jerzykiewicz (2003) showed that this problem may be solved by postulating the existence of a 5 to 10 kG magnetic field in the outer envelope of the star. From the campaign data (see Paper III), one gets $A = (-4.9 \pm 1.1) \times 10^{-4}$ $d^{-1}$, a value which is not in serious conflict with the observed $S$. Unfortunately, the large standard deviation of this result makes it useless. A longer time base-line than that of the 2002-3 campaign would be needed to obtain a more reliable value of $A$ and thus decide whether invoking magnetic field were necessary. This was one motivation for undertaking the sequel campaign.

In Paper III, the spherical harmonic degree of the $i = 5$, 6 and 7 terms was found to be $\ell = 1$, but an attempt to derive $\ell$ for the low-frequency $i =$ A term (referred to as the $\nu_{10}$ term in that paper) was unsuccessful because of its small *uvy* amplitudes and the poor resolution of diagnostic diagrams at low frequencies. Pamyatnykh et al. (2004) showed that the $i = 5$ term is a $p_2$ mode, while the $i = 6$ one is a $p_1$ mode. Moreover, they suggested that the low-frequency term is an $\ell = 1$, $m = -1$, $g_{16}$ mode.

According to Pamyatnykh et al. (2004), only the $i = 1$, 2, 3 and 4 modes (i.e., the radial fundamental mode and the $\ell = 1$, $g_1$ triplet) are unstable in standard models. Modes with $f > 6$ $d^{-1}$ (i.e., the $i = 5$, 6 and 7 ones) and the low-frequency mode are stable. Pamyatnykh et al. (2004) demonstrate, however, that a fourfold overabundance of Fe in the driving zone would account for excitation of the high-frequency modes, and would make the low-frequency mode marginally unstable.

It has been noted in Paper I that if the low-frequency term were indeed a high-order $g$ mode, $\nu$ Eri would be both a $\beta$ Cephei variable and a slowly pulsating (SPB) star. Unfortunately, $f_A$ differs from the sixth order combination frequency $3f_1 - 3f_3$ by less than 0.003 $d^{-1}$. This number is much larger than the formal error of $f_A$, but is smaller than half the frequency resolution of the campaign data. Thus, the possibility that $f_A$ is the combination frequency—although rather unlikely—cannot be rejected. Again, a longer time base-line would help to settle the issue.

In addition to extending the time base-line, the sequel campaign was expected to double the number of data points and thus lower the detection threshold so that modes having amplitudes too low to be seen in the 2002-3 frequency spectra could be discovered from the combined data.

Both comparison stars used in the 2002-3 photometric observations turned out to be variable. For the first, $\mu$ Eri (HD 30211, B5 IV, $V = 4.00$), the analysis carried out in Paper I revealed a dominant frequency $f_1' = 0.6164$ $d^{-1}$. (From now on we shall use a prime to denote frequencies of $\mu$ Eri.) Prewhitening with this frequency resulted in an amplitude spectrum with a very strong $1/f$ component, indicating a complex variation. Since the star is a spectroscopic binary with an orbital period $P_{orb} = 7.35890$ d (Hill 1969), tests have been made to detect a non-sinusoidal signal with this period. Unfortunately, they were inconclusive.

Taking into account the star's position in the HR diagram, the frequency $f_1'$ of the dominant variation, and the fact that the $u$ amplitude was about a factor of two greater than the $v$ and $y$ amplitudes, it was concluded in Paper I that $\mu$ Eri is probably an SPB star. However, it was also noted that instead of pulsation, a rotational modulation could be the cause of the dominant variation.

In Paper I, the frequency analysis of de-trended differential magnitudes of $\mu$ Eri revealed a small-amplitude variation with a frequency $f_x = 10.873$ $d^{-1}$. It was suggested that the second comparison star, $\xi$ Eri (HD 27861, A2 V, $V = 5.17$), may be responsible.

The present paper reports the sequel photometric campaign, carried out from 11 Sept. 2003 to 16 Feb. 2004, and an analysis of the data of both campaigns. The 2003-4 observations and reductions are described in Sect. 2. Sect. 3 contains an account of the frequency analysis of the new data and a comparison of the results with those of Paper I. Low frequencies in the variation of $\mu$ and $\nu$ Eri from the *uvy*

data of the first campaign are re-examined in Sect. 4. Sect. 5 is devoted to frequency analysis of the combined, 2002-4 data. Finally, Sect. 6 provides a summary with an emphasis on clues for asteroseismology of the three stars, $\nu$, $\mu$ and $\xi$ Eri.

## 2 OBSERVATIONS AND REDUCTIONS

The observations were carried out with five telescopes on four continents. An observing log is presented in Table 1. Comparison of this table with Table 1 of Paper I shows that the new data are almost as extensive as the old ones. However, the 2003-4 $y$ data are less numerous than the $v$ and $u$ ones (see below). The time base-lines of the 2002-3 and 2003-4 sets are very nearly the same; they amount to 157.9 and 158.5 d for the old and new data, respectively.

The five telescopes and photometers were the same as those in the 2002-3 campaign. Thus, single-channel photoelectric photometers were used at all sites but Sierra Nevada Observatory (OSN), where a simultaneous *uvby* photometer was used. At OSN, the observations were obtained with all four Strömgren filters, at Fairborn, Lowell and Siding Spring, with $u$, $v$ and $y$. At SAAO, the $y$ filter used in the 2002-3 campaign has deteriorated to such a degree that it had to be discarded. Since no replacement was available, the data were taken with two filters, Strömgren $u$ and $v$, except that on his first two nights AP used Johnson filters B and V.

The comparison stars and observing procedures were the same as in the first campaign.

The reductions, carried out separately for each of the three wavelength bands, $u$, $v$, and $y$ or $V$, consisted in (1) computing heliocentric JD numbers for the mean epochs of observations, (2) computing the air mass for each observation, (3) correcting instrumental magnitudes of $\nu$, $\mu$ and $\xi$ Eri for atmospheric extinction with first-order extinction coefficients derived from the instrumental magnitudes of $\xi$ Eri by means of Bouguer plots, (4) forming differential magnitudes '$\nu$ Eri $-$ $\xi$ Eri' and '$\mu$ Eri $-$ $\xi$ Eri,' and (5) setting the mean light-levels of the differential magnitudes from different telescope-filter combinations to the same values. In step 3, second-order extinction corrections were not applied because no colour-dependent extinction effects could be detected in the uncorrected differential magnitudes (but see the last paragraph of Sect. 3.1). In step 4, the magnitudes of $\xi$ Eri were interpolated on the epoch of observation of $\nu$ or $\mu$ Eri. In step 5, the mean-light levels for each telescope-filter combination were derived using residuals from least-squares solutions with the four highest-amplitude terms (see the Introduction).

## 3 FREQUENCY ANALYSIS OF THE NEW DATA

The analysis was carried out in essentially the same way as in Paper I. That is, frequencies were identified from periodograms, one at a time. Before each run, the data were prewhitened with all frequencies found in previous runs. After several runs, the frequencies were refined by means of a nonlinear least-squares fit using the values of independent frequencies read off the periodograms as starting values. The frequencies of the combination terms were computed from the independent frequencies. Thus, the unknowns in the normal equations were the corrections to the independent frequencies, to the mean magnitude, $\langle\Delta m\rangle$, and to the amplitudes, $A_i$, and phases, $\phi_i$, appearing in the following expression:

$$\Delta m = \langle\Delta m\rangle + \sum_{i=1}^{N} A_i \sin[2\pi f_i(t-t_0)+\phi_i], \qquad (3)$$

where $\Delta m$ is the differential magnitude in $u$, $v$, or $yV$, $N$ is the number of all frequencies, $f_i$, the combination terms included, and $t_0$ is an arbitrary initial epoch.

The difference with respect to the 2002-3 analysis consisted in using different programs: the PERIOD 98 package (see Paper I) was replaced with programs that have been in use by MJ since 1975 (see, e.g., Jerzykiewicz 1978). Thus, by "periodogram" we now mean a power spectrum, and not an amplitude spectrum as in Paper I; by "power" we mean $1-\sigma^2(f)/\sigma^2$, where $\sigma^2(f)$ is the variance of a least-squares fit of a sine-curve of frequency $f$ to the data, and $\sigma^2$ is the variance of the same data. However, for the purpose of estimating signal-to-noise ratios (see below) we also computed amplitude spectra.

### 3.1 The programme star

The data used for analysis were the differential magnitudes '$\nu$ Eri $-$ $\xi$ Eri.' Power spectra were computed independently from the $u$ and $v$ data. No power spectra were computed from the less numerous $yV$ data, but nonlinear least-squares solutions were carried out for all three bands, with the starting values of the independent frequencies for $y$ (henceforth we shall use "$y$" instead of "$yV$") taken from $v$. The OSN $b$ and SAAO $B$ data were not used.

In the $u$ and $v$ power spectra, 14 independent and 15 combination frequencies could be clearly seen. They are identified in the first column of Table 2. The numbers in the table are from nonlinear least-squares solutions. The values of the independent frequencies and their standard deviations, computed as straight means from the separate solutions for $u$, $v$ and $y$, are given in column 2 above the horizontal line. The combination frequencies, listed below the line, were computed from the independent frequencies according to ID in the first column; their standard deviations were computed from the standard deviations of the independent frequencies assuming rms propagation of errors. The amplitudes, $A_u$, $A_v$ and $A_y$, with the standard deviations, given in columns 3, 4 and 5, respectively, are from the independent solutions for $u$, $v$ and $y$. The last column lists the $v$-amplitude signal-to-noise ratio, $S/N$, defined as in Paper I, except that in Paper I the mean noise level was estimated in 5 $\mathrm{d}^{-1}$ intervals, while now we adopted 0.1 $\mathrm{d}^{-1}$ intervals for frequencies lower than 3 $\mathrm{d}^{-1}$, and 1 $\mathrm{d}^{-1}$ for higher frequencies. In all cases, the amplitude spectra of the data prewhitened with the 29 frequencies of Table 2 were used for estimating the mean noise level.

In Paper I, a peak in the amplitude spectrum was considered to be significant if its signal-to-noise ratio exceeded 4 for an independent term or 3.5 for a combination term. As can be seen from Table 2, this condition is met by all

**Table 1.** Log of the photometric measurements of $\nu$ Eri in 2003-4. Observatories are listed in the order of their geographic longitude.

| Observatory | Longitude | Latitude | Telescope | Amount of data Nights | h | Observer(s) |
|---|---|---|---|---|---|---|
| Sierra Nevada Observatory | $-3^\circ 23'$ | $+37^\circ 04'$ | 0.9-m | 4 | 10.64 | ER |
| Fairborn Observatory | $-110^\circ 42'$ | $+31^\circ 23'$ | 0.75-m APT | 51 | 211.09 | −− |
| Lowell Observatory | $-111^\circ 40'$ | $+35^\circ 12'$ | 0.5-m | 25 | 87.10 | MJ |
| Siding Spring Observatory | $+149^\circ 04'$ | $-31^\circ 16'$ | 0.6-m | 26 | 79.77 | RRS |
| South African Astronomical Observatory | $+20^\circ 49'$ | $-32^\circ 22'$ | 0.5-m | 17 | 92.13 | AP |
| South African Astronomical Observatory | $+20^\circ 49'$ | $-32^\circ 22'$ | 0.5-m | 19 | 48.52 | RM, TM, PT |
| Total | | | | 142 | 529.25 | |

**Table 2.** Frequencies and amplitudes in the differential magnitudes '$\nu$ Eri − $\xi$ Eri' from the 2003-4 data. Independent frequencies are listed in the upper part of the table. The combination frequencies are listed below the horizontal line. In both cases the frequencies are ordered according to decreasing $v$ amplitude, $A_v$. The last column contains the $v$-amplitude signal-to-noise ratio. Frequencies $f_{\rm x}$ and $f_{\rm y}$ are due to $\xi$ Eri.

| ID | Frequency [d$^{-1}$] | $A_u$ [mmag] | $A_v$ [mmag] | $A_y$ [mmag] | $S/N$ |
|---|---|---|---|---|---|
| $f_1$ | 5.763256 ± 0.000012 | 72.3 ± 0.19 | 40.6 ± 0.14 | 36.7 ± 0.15 | 165.0 |
| $f_2$ | 5.653897 ± 0.000020 | 38.6 ± 0.19 | 27.2 ± 0.14 | 25.4 ± 0.15 | 110.6 |
| $f_3$ | 5.619979 ± 0.000021 | 35.5 ± 0.19 | 25.0 ± 0.14 | 24.0 ± 0.15 | 101.6 |
| $f_4$ | 5.637215 ± 0.000025 | 31.0 ± 0.18 | 21.8 ± 0.13 | 20.4 ± 0.16 | 88.6 |
| $f_5$ | 7.89859 ± 0.00022 | 3.7 ± 0.19 | 2.7 ± 0.14 | 2.5 ± 0.16 | 11.0 |
| $f_7$ | 6.26225 ± 0.00025 | 3.1 ± 0.19 | 2.2 ± 0.14 | 2.2 ± 0.16 | 8.8 |
| $f_{\rm A}$ | 0.43257 ± 0.00028 | 3.2 ± 0.19 | 2.0 ± 0.14 | 1.7 ± 0.16 | 5.0 |
| $f_6$ | 6.24468 ± 0.00034 | 2.3 ± 0.18 | 1.6 ± 0.13 | 1.6 ± 0.15 | 6.4 |
| $f_{\rm B}$ | 0.61411 ± 0.00033 | 3.4 ± 0.18 | 1.5 ± 0.13 | 1.6 ± 0.15 | 4.3 |
| $f_{\rm x}$ | 10.8743 ± 0.0006 | 1.2 ± 0.18 | 1.4 ± 0.13 | 0.9 ± 0.15 | 5.7 |
| $f_{10}$ | 7.9296 ± 0.0005 | 1.6 ± 0.19 | 1.2 ± 0.14 | 1.2 ± 0.16 | 5.3 |
| $f_9$ | 7.9132 ± 0.0005 | 1.8 ± 0.18 | 1.1 ± 0.13 | 1.3 ± 0.16 | 4.9 |
| $f_8$ | 7.2006 ± 0.0005 | 1.4 ± 0.18 | 1.0 ± 0.13 | 1.1 ± 0.15 | 4.4 |
| $f_{\rm y}$ | 17.2534 ± 0.0006 | 1.0 ± 0.19 | 0.9 ± 0.13 | 0.9 ± 0.15 | 4.6 |
| $f_1 + f_2$ | 11.417153 ± 0.000023 | 12.3 ± 0.19 | 8.8 ± 0.14 | 8.4 ± 0.15 | 34.0 |
| $f_1 + f_3$ | 11.383235 ± 0.000024 | 10.8 ± 0.19 | 7.6 ± 0.14 | 7.1 ± 0.15 | 29.3 |
| $f_1 + f_4$ | 11.400471 ± 0.000028 | 9.9 ± 0.19 | 7.0 ± 0.14 | 6.6 ± 0.16 | 27.0 |
| $2f_1$ | 11.526512 ± 0.000017 | 4.5 ± 0.18 | 3.1 ± 0.13 | 3.1 ± 0.15 | 12.0 |
| $f_1 + f_2 + f_3$ | 17.037132 ± 0.000031 | 3.3 ± 0.18 | 2.2 ± 0.13 | 2.0 ± 0.15 | 11.3 |
| $f_1 - f_2$ | 0.109359 ± 0.000023 | 2.7 ± 0.19 | 1.6 ± 0.14 | 1.6 ± 0.16 | 4.4 |
| $2f_1 + f_4$ | 17.163727 ± 0.000030 | 1.9 ± 0.18 | 1.4 ± 0.13 | 1.3 ± 0.15 | 7.2 |
| $2f_1 + f_2$ | 17.180409 ± 0.000026 | 1.9 ± 0.18 | 1.4 ± 0.13 | 1.3 ± 0.15 | 7.2 |
| $f_2 + f_3$ | 11.273876 ± 0.000029 | 2.4 ± 0.19 | 1.3 ± 0.14 | 1.1 ± 0.15 | 5.0 |
| $2f_1 + f_3$ | 17.146491 ± 0.000027 | 1.4 ± 0.18 | 1.2 ± 0.13 | 0.8 ± 0.15 | 6.2 |
| $2f_2$ | 11.307794 ± 0.000028 | 1.1 ± 0.19 | 1.1 ± 0.14 | 0.6 ± 0.16 | 4.2 |
| $f_1 - f_4$ | 0.126041 ± 0.000028 | 1.9 ± 0.18 | 1.1 ± 0.13 | 1.2 ± 0.15 | 3.0 |
| $f_1 + f_3 + f_4$ | 17.020450 ± 0.000035 | 1.3 ± 0.18 | 1.1 ± 0.13 | 0.9 ± 0.15 | 5.6 |
| $2f_1 + f_2 + f_3$ | 22.800388 ± 0.000034 | 1.3 ± 0.18 | 1.1 ± 0.13 | 0.8 ± 0.15 | 6.1 |
| $f_1 + f_2 - f_3$ | 5.797174 ± 0.000031 | 1.5 ± 0.19 | 0.9 ± 0.14 | 1.3 ± 0.15 | 3.7 |

terms identified from the 2003-4 data except the differential combination term $f_1 - f_4$ for which $S/N = 3.0$. This term may be spurious.

The standard deviations in Table 2 (and in the tables that follow), referred to as "formal" in the remainder this subsection and in the first three paragraphs of the next subsection, will be underestimated if the errors of differential magnitudes are correlated in time. For the case at hand, i.e., of fitting a sinusoid to time series data, the problem has been discussed by Schwarzenberg-Czerny (1991) and Montgomery & O'Donoghue (1999). These authors consider the factor, $D$, by which the formal standard deviations of a frequency, amplitude and phase should be multiplied in order to get correct values. ($D$ is the same for frequencies, amplitudes and phases because the ratio of the formal standard deviations of any two of these quantities is determined by error-free numbers such as the epochs of observations and the starting values of the frequencies.) The factor depends on

an estimate of the number of consecutive data points which are correlated. Unfortunately, this estimate is not easy to obtain, especially for time series such as ours, consisting of data from many nights and several observatories. We shall return to this point in the next subsection.

Figure 1 shows the power spectra of the $u$ and $v$ differential magnitudes '$\nu$ Eri $-$ $\xi$ Eri' prewhitened with the 29 frequencies of Table 2. In both panels of the figure, the highest peaks are seen at frequencies lower than about 5 $d^{-1}$. In the $u$ spectrum (lower panel), the highest peak occurs at 0.314 $d^{-1}$, while in the $v$ spectrum, the highest peak is the one at 1.498 $d^{-1}$. The $u$ amplitude at 0.314 $d^{-1}$ is equal to 2.2 mmag, while the $v$ amplitude at 1.498 $d^{-1}$, to 1.1 mmag. The $u$- and $v$-amplitude $S/N$ amount to 2.7 in both cases. We conclude that these frequencies are probably spurious.

For frequencies higher than 5 $d^{-1}$, the highest peak in the $u$ spectrum (lower panel) occurs at 5.015 $d^{-1}$. For this peak the $u$-amplitude $S/N$ is equal to 5.0, so that the significance condition mentioned earlier in this section is satisfied. However, there is no power at 5.015 $d^{-1}$ in the $v$ spectrum (upper panel); the peak closest to 5.015 $d^{-1}$, at 5.128 $d^{-1}$, is probably noise because it has $S/N$ equal to 3.2. This, and the fact that 5.015 $d^{-1}$ is very nearly equal to 5 cycles per sidereal day ($sd^{-1}$), suggest that the peak is due to colour extinction in the $u$ band which we neglected (see Sect. 2). Indeed, the differential colour-extinction correction contains a term equal to $k''X\Delta C$, where $k''$ is the scond-order extinction coefficient, $X$ is the air-mass, and $\Delta C$ is the differential colour-index. Because of the second factor, $X$, the term causes a parabola-shaped variation symmetrical around the time of meridian passage. For a single observatory, this will produce a signal with frequency equal to $n$ $sd^{-1}$, where $n$ is a small whole number equal to the number of sinewaves that best fit the variations on successive nights. In our case this number is apparently equal to 5. For multi-site data, phase smearing may occur, tending to wash out the signal. However, our time-series is dominated by the data from Fairborn and Lowell, two observatories lying on nearly the same meridian and therefore introducing negligible phase shift. In addition, the greatest common divisor of the longitude differences between Fairborn and Lowell on one hand, and SAAO and Siding Spring on the other is close to $60^o$, making the 5 $sd^{-1}$ signals from these observatories to approximately agree in phase. We conclude that the 5.015 $d^{-1}$ peak in the $u$ spectrum in Fig. 1 is not due to an intrinsic variation of $\nu$ Eri.

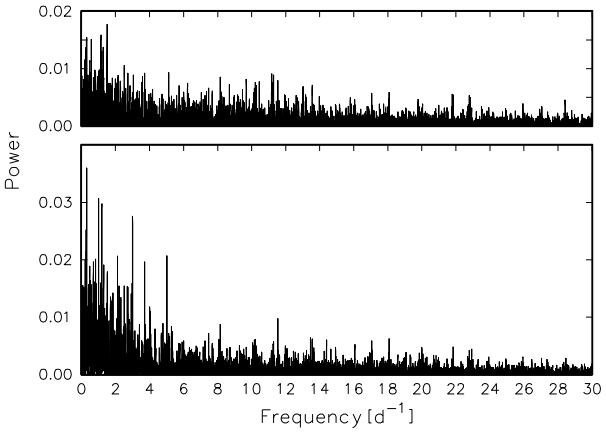


**Figure 1.** Power spectra of the $u$ (lower panel) and $v$ (upper) differential magnitudes '$\nu$ Eri $-$ $\xi$ Eri' prewhitened with the 29 frequencies of Table 2.

### 3.2 Comparison of the 2003-4 and 2002-3 results for the programme star

Of the 14 independent terms in Table 2, nine appear in Table 2 of Paper I. The differences between the 2003-4 and 2002-3 values of their frequencies and amplitudes are listed in Table 3. The standard deviations given in the table were computed from the standard deviations of the 2003-4 and 2002-3 least-squares solutions assuming rms propagation of errors. Thus, they are formal in the sense defined in the previous subsection.

We shall now return to the factor $D$ by which the formal standard deviations are underestimated. Let us consider the nine independent frequencies common to 2002-3 and 2003-4. As can be seen from Table 3, the moduli of the frequency differences, $|\Delta f|$, are of the same order of magnitude as the formal standard deviations of $\Delta f$, $\sigma_{\Delta f}$. In four cases $|\Delta f| < \sigma_{\Delta f}$, in three cases $\sigma_{\Delta f} < |\Delta f| < 2\sigma_{\Delta f}$, and in two cases the differences exceed $2\sigma_{\Delta f}$. Taken at face value, these inequalities would indicate that four or five of the nine frequencies changed from 2002-3 to 2003-4 by $1\sigma_{\Delta f}$ or more, while $f_3$, $f_5$ and $f_8$ changed by $2\sigma_{\Delta f}$ or more. However, frequency changes in $\beta$ Cephei stars have time scales much longer than 1 year. For the four first frequencies of $\nu$ Eri, this is shown to be the case by Handler et al. (2005). Although the existence of long-term variations does not exclude the possibility of year-to-year ones, let us assume that these four frequencies were strictly constant from 2002 to 2004. If the assumption were false, the value of $D$ we derive in the next paragraph will be too large.

For $f = const$, where $f$ is any of the four frequencies, the modulus of $\Delta f$ can be thought of as the range of $f$ in a two-element sample of $f$, the first element chosen from the parent population of $f$ in 2002-3, and the second element chosen from the same population in 2003-4. For a normal distribution, an estimate of the standard deviation can be obtained by multiplying the range by a coefficient $k$ which is a function of the number of elements in the sample, $n$. For $n = 2$, Table 12 of Crow, Davis & Maxfield (1960) reads $k = 0.886$. Multiplying $|\Delta f|$ by this value we get an estimate of the standard deviation of $f$. The latter number divided by the formal standard deviation of $f$ from Table 2 yields the factor we are seeking. The mean value of the factor for the four frequencies turns out to be $D = 2.0$. If we applied the procedure to all nine frequencies, the result would be $D = 1.8$. If we used the formal standard deviations of the 2002-3 solution, the results would be very nearly the same. Henceforth we shall adopt $D = 2$. A standard deviation equal to the formal standard deviation times this factor we shall refer to as "corrected," and from now on we shall drop the adjective "formal," so that by "standard deviation" we shall mean "formal standard deviation."

Multiplying the standard deviations of the 2003-4 amplitudes by two, we find that the ratios of the amplitudes to the corrected standard deviations become approximately equal to the signal-to-noise ratios defined in the previous subsection. This is a pleasant surprise, lending support to

**Table 3.** A comparison of the frequencies and amplitudes of the nine independent terms common to Table 2 of Paper I and Table 2 of the present paper. The differences, $\Delta$, are in the sense '2003-4 *minus* 2002-3.'

| ID | $\Delta f$ [d$^{-1}$] | $\Delta A_u$ [mmag] | $\Delta A_v$ [mmag] | $\Delta A_y$ [mmag] |
|---|---|---|---|---|
| $f_1$ | $-0.000014 \pm 0.000017$ | $-1.2 \pm 0.27$ | $-0.4 \pm 0.20$ | $-0.2 \pm 0.20$ |
| $f_2$ | $-0.000033 \pm 0.000028$ | $0.7 \pm 0.27$ | $0.8 \pm 0.20$ | $0.3 \pm 0.20$ |
| $f_3$ | $-0.000081 \pm 0.000030$ | $0.9 \pm 0.27$ | $1.0 \pm 0.20$ | $1.3 \pm 0.20$ |
| $f_4$ | $0.000055 \pm 0.000035$ | $-1.2 \pm 0.27$ | $-0.6 \pm 0.20$ | $-0.6 \pm 0.20$ |
| $f_5$ | $0.00079 \pm 0.00032$ | $-0.6 \pm 0.27$ | $-0.4 \pm 0.20$ | $-0.5 \pm 0.20$ |
| $f_6$ | $0.00060 \pm 0.00048$ | $-1.6 \pm 0.27$ | $-0.9 \pm 0.20$ | $-1.0 \pm 0.20$ |
| $f_7$ | $0.00020 \pm 0.00035$ | $0.2 \pm 0.27$ | $0.3 \pm 0.20$ | $0.4 \pm 0.20$ |
| $f_8$ | $0.00066 \pm 0.00071$ | $0.1 \pm 0.27$ | $0.1 \pm 0.20$ | $0.0 \pm 0.20$ |
| $f_A$ | $0.00039 \pm 0.00040$ | $-2.3 \pm 0.27$ | $-1.2 \pm 0.20$ | $-1.5 \pm 0.20$ |

our value of $D$. (Using the numbers from Table 2, the reader can verify the approximate equality of $S/N$ and $A_v/(2\sigma_v)$, where $\sigma_v$ is the standard deviation of $A_v$. Note that while for low frequencies $A_v/(2\sigma_v)$ is about 30% larger than $S/N$, the approximate equality improves for high frequencies. This seems to be reasonable in view of the $1/f$ decrease of the noise level in the periodograms.) Additional support for $D = 2$ comes from the fact that a different line of reasoning applied to multisite data similar to ours has led Handler et al. (2000) to the same value.

Let us now return to Table 3. As can be seen from the table, $|\Delta A|$ are the largest for $f_A$, $f_6$, and $f_3$ (in this order). Multiplying the standard deviations of $\Delta A$ by $D = 2$ we find that (1) the amplitude of the low frequency term has decreased by $4.3\sigma_c$ in $u$, $3.0\sigma_c$ in $v$, and $3.8\sigma_c$ in $y$, where by $\sigma_c$ we denote the corrected standard deviation of $\Delta A$, (2) the amplitude of the $i = 6$ term has decreased by 3.0, 2.2, and $2.5\sigma_c$ in $u$, $v$, and $y$, respectively, and (3) the amplitude of the $i = 3$ term has increased by 1.7, 2.5, and $3.2\sigma_c$ in $u$, $v$, and $y$, respectively. For the remaining six terms, $|\Delta A| \leqslant 2.2\sigma_c$. We conclude that the decrease of the amplitude of the $i = A$ term is real, that of the $i = 6$ term may be real, while the amplitude increase of the $i = 3$ term is probably spurious. In the remaining cases, there is little or no evidence for amplitude variation.

The five independent frequencies which appear in the present Table 2 but not in Table 2 of Paper I are (in the order of decreasing $v$ amplitude) $f_B$, $f_x$, $f_{10}$, $f_9$, $f_y$. The low frequency $f_B$ is very nearly equal to the frequency $f_{21}$, one of three low frequencies derived in Paper II from the radial velocities of $\nu$ Eri. However, in our 2003-4 power spectra we did not see the other two low frequencies of Paper II. Frequency $f_9$ was listed in Table 3 of Paper I as that of one of several "possible further signals." Frequencies $f_{10}$ and $f_y$ are new.

Frequency $f_x$ was found in Paper I and tentatively ascribed to $\xi$ Eri (see the Introduction). We shall demonstrate in Sect. 3.3 that this frequency and $f_y$, the smallest-amplitude independent frequency in Table 2, are both due to $\xi$ Eri.

In addition to nine independent terms, Table 2 of Paper I lists 14 combination terms. In the 2003-4 power spectra we did not see three of them, viz., $f_1 + f_5$, $f_1 + f_2 + f_4$ and $f_1 + 2f_2$. On the other hand, we detected differential combination-terms $f_1 - f_2$, $f_1 + f_2 - f_3$ and $f_1 - f_4$ which were not found in Paper I.

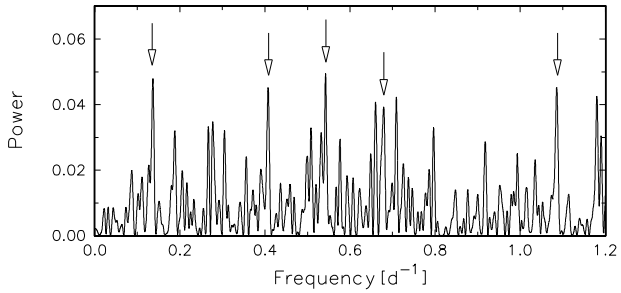


**Figure 2.** Low-frequency part of the power spectrum of the $v$ differential magnitudes '$\mu$ Eri $-$ $\xi$ Eri' prewhitened with 0.615 d$^{-1}$, $2f'_{\rm orb}$ and $6f'_{\rm orb}$. Arrows indicate peaks at frequencies equal to $f'_{\rm orb}$, $3f'_{\rm orb}$, $4f'_{\rm orb}$, $5f'_{\rm orb}$ and $8f'_{\rm orb}$.

### 3.3 The comparison stars

The data used for analysis were the differential magnitudes '$\mu$ Eri $-$ $\xi$ Eri.' Power spectra were computed independently from the $u$ and $v$ data. No power spectra were computed from the less numerous $y$ data.

In the first-run $u$ and $v$ power spectra, the highest peaks occurred at the same frequency of 0.615 d$^{-1}$. This frequency is close to $f'_1$, the only one found for $\mu$ Eri in Paper I (see the Introduction). The second and third runs yielded frequencies of 0.272 and 0.815 d$^{-1}$, again the same for $u$ and $v$. The first of these numbers is close to twice the orbital frequency of $\mu$ Eri, $f'_{\rm orb} = 0.13589$ d$^{-1}$, while the second, to six times this frequency. The low-frequency part of the power spectrum of the $v$ differential magnitudes '$\mu$ Eri $-$ $\xi$ Eri' prewhitened with 0.615 d$^{-1}$, $2f'_{\rm orb}$ and $6f'_{\rm orb}$ is shown in Fig. 2. In this figure, the arrows indicate peaks at frequencies equal to $f'_{\rm orb}$, $3f'_{\rm orb}$, $4f'_{\rm orb}$, $5f'_{\rm orb}$ and $8f'_{\rm orb}$. Peaks at these frequencies are also present in the $u$ power-spectrum.

The occurrence of so many harmonics of the orbital frequency implies that the data contain a strongly non-sinusoidal signal of this frequency. The first possibility that comes to mind is an eclipse. Fig. 3, in which the differential magnitudes '$\mu$ Eri $-$ $\xi$ Eri' prewhitened with 0.615 d$^{-1}$ are

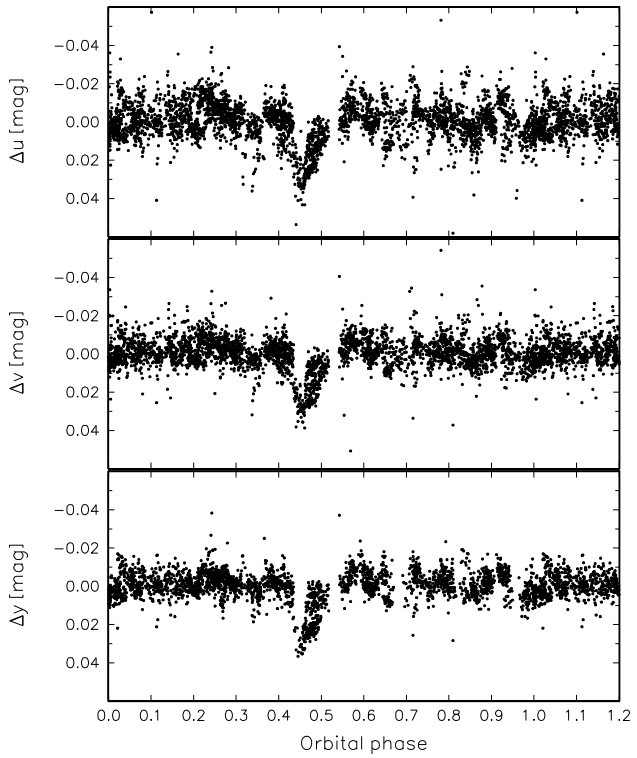


**Figure 3.** The $u$ (top), $v$ (middle) and $y$ (bottom) differential magnitudes '$\mu$ Eri − $\xi$ Eri' prewhitened with $f_1'$ are shown as a function of orbital phase of $\mu$ Eri. Phase zero corresponds to HJD 2452800.

plotted as a function of orbital phase, shows that $\mu$ Eri is indeed an eclipsing variable.

Returning to frequency analysis of the comparison-stars data, we rejected observations falling in the orbital phase range from 0.4 to 0.54, i.e., the data affected by the eclipse, and recomputed the power spectra. In the first-run $u$ and $v$ power-spectra, the highest peaks occurred at the same frequency of 0.615 d$^{-1}$ as before. The highest peaks in the second and third $u$ run were at 0.701 and 0.813 d$^{-1}$, respectively, while the second and third $v$ runs yielded 1.206 and 0.701 d$^{-1}$.

In the next step, we carried out nonlinear least-squares solutions separately for the $u$, $v$ and $y$ data. As starting values, we used all four frequencies found above, i.e., 0.615, 0.701, 0.8132 and 1.206 d$^{-1}$. The results are presented in the first four lines of Table 4. The fifth frequency, $f_5'$, will be explained shortly. The frequencies and their standard deviations, listed in column 2, were computed as straight means from the separate solutions for the three bands. The amplitudes, $A_u$, $A_v$ and $A_y$, and their standard deviations, are given in columns 4, 5 and 6. The $v$-amplitude signal-to-noise ratio, computed in the same way as in Sect. 3.1, is listed in the last column.

In the power spectra of the $u$ and $v$ differential magnitudes '$\mu$ Eri − $\xi$ Eri' prewhitened with the first four frequencies of Table 4, the highest peaks occur at the same frequency of 0.659 d$^{-1}$. Since a term of very nearly the same frequency is prominent in the frequency spectra of the 2002-3 comparison-stars data (see Sect. 4.2), we conclude that the signals at 0.659 d$^{-1}$ are intrinsic. A five-frequency nonlinear least-squares solution yielded the value of the fifth frequency and the corresponding amplitudes given in the last line of Table 4.

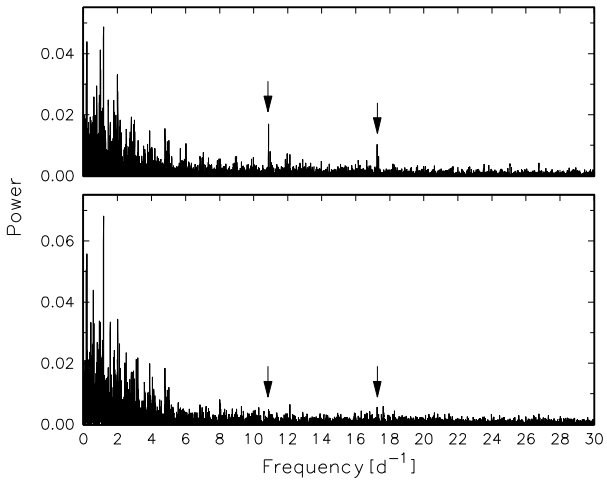


**Figure 4.** Power spectra of the $u$ (lower panel) and $v$ (upper) out-of-eclipse differential magnitudes '$\mu$ Eri − $\xi$ Eri' prewhitened with the five frequencies of Table 4. Arrows indicate frequencies $f_x = 10.874$ and $f_y = 17.254$ d$^{-1}$.

The power spectra of the $u$ and $v$ differential magnitudes '$\mu$ Eri − $\xi$ Eri' prewhitened with the five frequencies of Table 4 are shown in Fig. 4. In both spectra the highest peak occurs at 1.182 d$^{-1}$. Although these peaks may represent another term in the variation of $\mu$ Eri, we shall terminate the analysis at this stage for fear of over-interpreting the data.

At high frequencies, peaks at $f_x = 10.874$ and $f_y = 17.254$ d$^{-1}$ can be clearly seen in the $v$ spectrum (Fig. 4, upper panel). The $v$-amplitude signal-to-noise ratio is equal to 5.2 and 4.4 for $f_x$ and $f_y$, respectively. Although in the $u$ spectrum in the lower panel the peaks at these frequencies are masked by noise, a closer examination shows that they are present. For $f_x$, the $u$, $v$ and $y$ amplitudes computed from the differential magnitudes '$\mu$ Eri − $\xi$ Eri' amount to $0.9 \pm 0.22$, $1.2 \pm 0.16$ and $1.0 \pm 0.16$ mmag (formal sigmas), respectively. To within one formal $\sigma$, these numbers agree with the $f_x$ amplitudes derived from the '$\nu$ Eri − $\xi$ Eri' differential magnitudes (see Table 2). For $f_y$, the $u$, $v$ and $y$ amplitudes computed from the differential magnitudes '$\mu$ Eri − $\xi$ Eri' are equal to $0.9 \pm 0.22$, $0.9 \pm 0.16$ and $0.7 \pm 0.16$ mmag, respectively. Again, there is a $1\sigma$ agreement with the amplitudes obtained from the '$\nu$ Eri − $\xi$ Eri' data (see Table 2). In addition, the phases agree to within $1\sigma$ in all cases. We conclude that both frequencies are due to an intrinsic variation of $\xi$ Eri.

## 4 LOW FREQUENCIES FROM THE 2002-3 DATA

### 4.1 The eclipse

We have to admit that in our original analysis of the 2002-3 data we missed the eclipse of $\mu$ Eri (see Paper I and the Introduction). Fig. 5 shows phase diagrams in which the 2002-3 differential magnitudes '$\mu$ Eri − $\xi$ Eri' prewhitened

**Table 4.** Frequencies, periods and amplitudes in the out-of-eclipse differential magnitudes '$\mu$ Eri − $\xi$ Eri' from the 2003-4 data. The last column contains the $v$-amplitude signal-to-noise ratio.

| ID | Frequency [d$^{-1}$] | Period [d] | $A_u$ [mmag] | $A_v$ [mmag] | $A_y$ [mmag] | $S/N$ |
|---|---|---|---|---|---|---|
| $f_1'$ | 0.61504 ± 0.00010 | 1.6259 ± 0.00026 | 9.4 ± 0.22 | 6.1 ± 0.17 | 5.7 ± 0.16 | 11.1 |
| $f_2'$ | 0.70160 ± 0.00027 | 1.4253 ± 0.00055 | 4.0 ± 0.22 | 2.4 ± 0.16 | 2.2 ± 0.15 | 3.9 |
| $f_3'$ | 0.81351 ± 0.00026 | 1.2292 ± 0.00039 | 3.3 ± 0.22 | 2.2 ± 0.17 | 2.5 ± 0.17 | 4.1 |
| $f_4'$ | 1.20739 ± 0.00027 | 0.8282 ± 0.00019 | 3.1 ± 0.23 | 2.3 ± 0.17 | 2.3 ± 0.16 | 6.0 |
| $f_5'$ | 0.65934 ± 0.00028 | 1.5167 ± 0.00064 | 3.4 ± 0.21 | 2.3 ± 0.16 | 2.4 ± 0.15 | 4.2 |

with $f_1'$ are plotted as a function of orbital phase. The eclipse can be seen clearly.

A comparison of the phase diagrams in Figs. 5 and 3 shows that while the middle of the eclipse in 2002-3 falls at a phase of about 0.30, in 2003-4 it does at about 0.47, indicating a problem with Hill's (1969) value of the orbital period. Assuming that Hill's value yields a correct cycle count between the first eclipse observed in 2002 and the last one in 2003, we arrive at the following ephemeris:

$$\text{Min. light} = \text{HJD}\,2452574.04\,(4) + E/0.135490\,(18), \qquad (4)$$

where $E$ is the number of cycles elapsed from the epoch given (which is that of the middle of the first eclipse we caught in 2002), and the numbers in parentheses are estimated standard deviations with the leading zeroes suppressed. The question why our photometric period differs from Hill's spectrographic one will be addressed in a forthcoming paper.

### 4.2 Analysis of the out-of-eclipse $\mu$ Eri data

In 2002-3 the numbers of differential magnitudes '$\mu$ Eri − $\xi$ Eri' in the three bands were nearly the same, amounting to 2823, 2830 and 2919 in $u$, $v$ and $y$, respectively. After we rejected observations falling within the eclipse, these numbers were reduced to 2597, 2603 and 2688, still sufficient for analysis. Using these reduced data, we computed power spectra separately for $u$, $v$ and $y$. The first two runs yielded the same frequencies of 0.616 and 0.701 d$^{-1}$ in all three bands. These frequencies are very nearly equal to $f_1'$ and $f_2'$ of Table 4. In the third run, the highest peak in the $u$ power-spectrum was at 0.657 d$^{-1}$, while in the $v$ and $y$ power-spectra the highest peaks were at the same frequency of 1.207 d$^{-1}$. The first of these numbers is close to $f_5'$, while the second is nearly identical with $f_4'$ (see Table 4).

The fourth run was, however, a disappointment. In the $u$ power-spectrum, the highest peak occurred at 1.000 d$^{-1}$, while in the $v$ and $y$ ones, at 0.032 d$^{-1}$. Since neither of these frequencies is likely to be intrinsic, we did not attempt to compute fifth-run power spectra.

The four frequencies found above, i.e., 0.616, 0.701, 1.207 and 0.657 d$^{-1}$ were used as starting values in a four-frequency nonlinear least-squares solutions. Justification for including $f_4'$ in the $u$ solution comes from the fact that a peak at this frequency is prominent in the fourth-run $u$ power-spectrum. Likewise, $f_5'$ was included in the $v$ and $y$ solutions because prominent peaks at this frequency can be seen in the fourth-run $v$ and $y$ power-spectra.

The results of the four-frequency solutions are given in Table 5 above the horizontal line. This table has the same format as Table 4. However, the $S/N$ (last column) was now computed from the $y$ data.

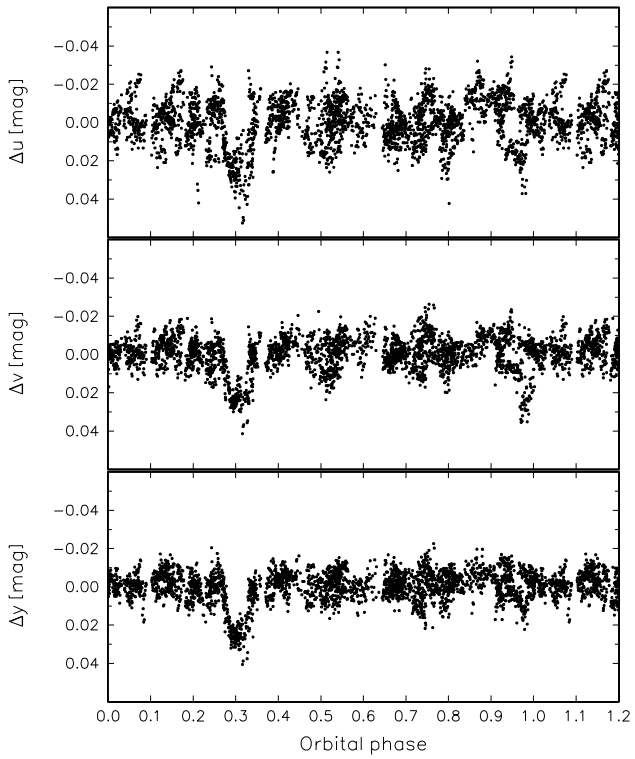


**Figure 5.** The $u$ (top), $v$ (middle) and $y$ (bottom) 2002-3 differential magnitudes '$\mu$ Eri − $\xi$ Eri' prewhitened with $f_1'$ are shown as a function of orbital phase of $\mu$ Eri. As in Fig. 3, phase zero corresponds to HJD 2452800.

The four-frequency solutions did not include $f_3'$. Since peaks at this frequency were present in the fourth-run $u$ and $v$ power-spectra, we carried out a five-frequency nonlinear least-squares solutions for all five frequencies of Table 4. The resulting values of $f_3'$, the amplitudes and $S/N$ are given in Table 5 below the horizontal line.

### 4.3 $\nu$ Eri

As explained in Paper I, the 2002-3 differential magnitudes of $\nu$ Eri were computed as '$\nu$ Eri *minus* the mean of comparison stars,' but with the low-frequency variations of $\mu$ Eri filtered out. Thus, a peak at low frequency in the power spectrum of these differential magnitudes—if not caused by

**Table 5.** Frequencies, periods and amplitudes in the out-of-eclipse differential magnitudes '$\mu$ Eri − $\xi$ Eri' from the 2002-3 data. The last column contains the $y$-amplitude signal-to-noise ratio.

| ID | Frequency [d$^{-1}$] | Period [d] | $A_u$ [mmag] | $A_v$ [mmag] | $A_y$ [mmag] | $S/N$ |
|---|---|---|---|---|---|---|
| $f_1'$ | 0.61587 ± 0.00013 | 1.62372 ± 0.00034 | 9.9 ± 0.26 | 6.2 ± 0.19 | 4.9 ± 0.15 | 9.4 |
| $f_2'$ | 0.70143 ± 0.00021 | 1.42566 ± 0.00043 | 6.9 ± 0.25 | 4.4 ± 0.19 | 3.3 ± 0.15 | 4.1 |
| $f_4'$ | 1.20690 ± 0.00030 | 0.82857 ± 0.00021 | 3.2 ± 0.25 | 3.4 ± 0.19 | 2.7 ± 0.15 | 4.5 |
| $f_5'$ | 0.65751 ± 0.00036 | 1.5209 ± 0.0008 | 4.2 ± 0.25 | 2.3 ± 0.19 | 2.2 ± 0.15 | 4.2 |
| $f_3'$ | 0.8147 ± 0.0006 | 1.2275 ± 0.0009 | 3.1 ± 0.24 | 2.3 ± 0.19 | 0.8 ± 0.15 | 1.4 |

noise—would be due to an intrinsic variation of $\nu$ or $\xi$ Eri. In the latter case, however, the peaks would be suppressed by a factor of four, while the corresponding amplitudes would be divided by two.

In Paper I we found a prominent peak at 0.254 d$^{-1}$ in the amplitude spectrum of the $v$ differential-magnitudes prewhitened with all 23 frequencies identified from the 2002-3 data. The power spectrum of the same data also shows a prominent peak at this frequency. However, there is little power at this frequency in the 2003-4 spectra shown in Fig. 1. On the other hand, in the 2002-3 $u$, $v$ and $y$ power-spectra there are peaks at 0.615 d$^{-1}$, a frequency very nearly equal to $f_{\rm B}$ found in Sect. 3.1 from the 2003-4 data. The 2002-3 $u$, $v$ and $y$ amplitudes at this frequency amount to $2.5 \pm 0.19$, $1.2 \pm 0.14$ and $1.4 \pm 0.12$ mmag, respectively, in fair agreement with the 2003-4 amplitudes listed in Table 2. Since multiplying the 2002-3 amplitudes by two would make the agreement much worse, the possibility that $f_{\rm B}$ is due to $\xi$ Eri can be rejected.

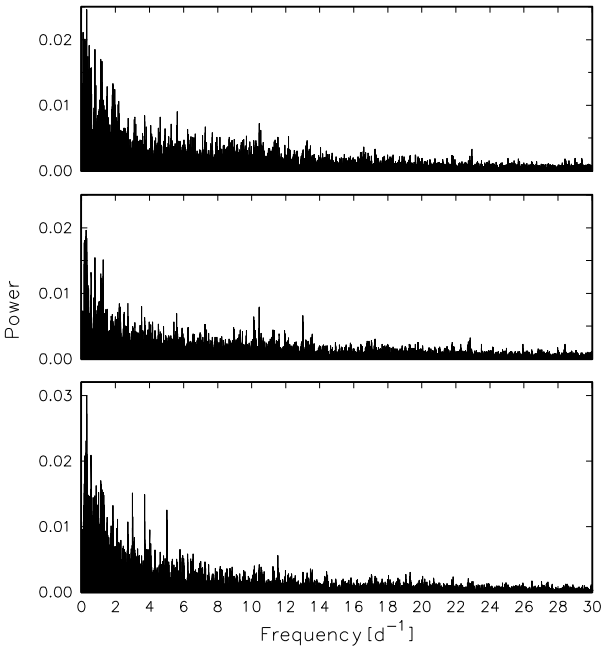


**Figure 6.** Power spectra of the combined, 2002-4 $u$ (bottom), $v$ (middle) and $y$ (top) differential magnitudes of $\nu$ Eri prewhitened with the 36 frequencies of Table 6.

## 5 ANALYSIS OF THE COMBINED DATA

### 5.1 $\nu$ Eri

After slight mean-light-level adjustments, the 2002-3 and 2003-4 differential magnitudes of $\nu$ Eri were combined, separately for $u$, $v$ and $y$. The combined, 2002-4 data have the time base-line of 525.8 d. The analysis of the 2002-4 differential magnitudes was carried out in the same way as that of the 2003-4 data (see Sect. 3). Sixteen independent and 20 combination frequencies could be identified from the power spectra. In all cases but two the yearly aliases were significantly lower than the central peak, so that there was no $\pm 1$ y$^{-1}$ uncertainty. This was to be expected because the 2002-3 and 2003-4 observing windows span as much as 0.43 y each (see Sect. 2). The two exceptions were $f_6$ and $f_{12}$. They will be discussed later in this section.

The 36 frequencies derived from the combined data are listed in the first column of Table 6. As in Tables 2, 4 and 5, the values of the independent frequencies and their standard deviations, given in column 2, were computed as straight means from the separate solutions for $u$, $v$ and $y$. The combination frequencies, listed below the horizontal line, were computed from the independent frequencies according to ID in the first column; their standard deviations were computed from the standard deviations of the independent frequencies assuming rms propagation of errors. The amplitudes, $A_u$, $A_v$ and $A_y$, given together with their standard deviations in columns 3, 4 and 5, respectively, are from the independent solutions for $u$, $v$ and $y$. The $v$-amplitude $S/N$, computed in the same way as in Sect. 3.1, is given in the last column. It can be seen that all independent frequencies meet the significance condition of Paper I. Among combination frequencies, this condition is not satisfied in two cases, viz., $f_3 + f_4$ and $f_1 - f_4$.

In addition to frequencies derived from the 2003-4 data (see Table 2), Table 6 contains two further high frequencies due to $\nu$ Eri, viz., $f_{11}$ and $f_{12}$. The latter is close to that of one of several "possible further signals" listed in Table 3 of Paper I and to frequency $\nu_7$ obtained in Paper III from radial velocities of the SiIII triplet around 457 nm. Frequency $f_{11}$ is new. In order to make sure that this frequency is not due to $\xi$ Eri, we examined the 2002-4 out-of-eclipse differential magnitudes '$\mu$ Eri − $\xi$ Eri' prewhitened with the six frequencies of Table 7 (see the next subsection). In the periodograms, there were no peaks at $f_{11}$; the highest peak in the vicinity, at 6.7168 d$^{-1}$, had the $v$ amplitude equal to about 0.4 mmag and $S/N < 2.5$. Analogous tests with the 2002-3 data also proved negative.

**Table 6.** Frequencies and amplitudes in the differential magnitudes of $\nu$ Eri from the combined 2002-2004 data. Independent frequencies are listed in the upper part of the table. The combination frequencies are listed below the horizontal line. In both cases the frequencies are ordered according to decreasing $v$ amplitude, $A_v$. Frequencies $f_{\rm x}$ and $f_{\rm y}$ are due to $\xi$ Eri.

| ID | Frequency [$d^{-1}$] | $A_u$ [mmag] | $A_v$ [mmag] | $A_y$ [mmag] | $S/N$ |
|---|---|---|---|---|---|
| $f_1$ | 5.7632828 ± 0.0000019 | 72.8 ± 0.13 | 40.8 ± 0.10 | 36.7 ± 0.10 | 214.7 |
| $f_2$ | 5.6538767 ± 0.0000030 | 38.5 ± 0.13 | 27.1 ± 0.10 | 25.4 ± 0.10 | 142.6 |
| $f_3$ | 5.6200186 ± 0.0000031 | 35.0 ± 0.13 | 24.5 ± 0.10 | 23.2 ± 0.10 | 129.0 |
| $f_4$ | 5.6372470 ± 0.0000038 | 31.8 ± 0.13 | 22.3 ± 0.10 | 21.0 ± 0.10 | 117.4 |
| $f_5$ | 7.898200 ± 0.000032 | 3.6 ± 0.13 | 2.6 ± 0.10 | 2.5 ± 0.10 | 14.5 |
| $f_{\rm A}$ | 0.432786 ± 0.000032 | 4.1 ± 0.13 | 2.5 ± 0.10 | 2.5 ± 0.10 | 8.3 |
| $f_7$ | 6.262917 ± 0.000044 | 2.8 ± 0.14 | 2.0 ± 0.10 | 1.8 ± 0.10 | 11.0 |
| $f_6$ | 6.243847 ± 0.000042 | 3.0 ± 0.13 | 1.9 ± 0.10 | 2.1 ± 0.10 | 10.5 |
| $f_B$ | 0.61440 ± 0.00005 | 3.0 ± 0.13 | 1.4 ± 0.10 | 1.6 ± 0.10 | 5.5 |
| $f_9$ | 7.91383 ± 0.00008 | 1.7 ± 0.13 | 1.1 ± 0.10 | 1.2 ± 0.10 | 6.1 |
| $f_{\rm x}$ | 10.87424 ± 0.00012 | 0.8 ± 0.13 | 1.0 ± 0.10 | 0.7 ± 0.10 | 5.7 |
| $f_{10}$ | 7.92992 ± 0.00010 | 1.2 ± 0.13 | 0.9 ± 0.10 | 0.9 ± 0.10 | 5.0 |
| $f_8$ | 7.20090 ± 0.00009 | 1.4 ± 0.13 | 0.9 ± 0.10 | 0.9 ± 0.10 | 5.0 |
| $f_{11}$ | 6.73223 ± 0.00012 | 1.0 ± 0.13 | 0.8 ± 0.10 | 0.6 ± 0.10 | 4.5 |
| $f_{12}$ | 6.22360 ± 0.00012 | 0.9 ± 0.13 | 0.8 ± 0.10 | 0.8 ± 0.10 | 4.4 |
| $f_{\rm y}$ | 17.25241 ± 0.00016 | 0.6 ± 0.13 | 0.6 ± 0.10 | 0.5 ± 0.10 | 4.4 |
| $f_1+f_2$ | 11.4171595 ± 0.0000036 | 12.4 ± 0.13 | 8.8 ± 0.10 | 8.4 ± 0.10 | 50.9 |
| $f_1+f_3$ | 11.3833014 ± 0.0000036 | 10.8 ± 0.14 | 7.6 ± 0.10 | 7.3 ± 0.10 | 44.0 |
| $f_1+f_4$ | 11.4005298 ± 0.0000042 | 10.2 ± 0.14 | 7.2 ± 0.10 | 6.8 ± 0.10 | 41.7 |
| $2f_1$ | 11.5265656 ± 0.0000027 | 4.4 ± 0.13 | 3.1 ± 0.10 | 2.9 ± 0.10 | 17.9 |
| $f_1+f_2+f_3$ | 17.037178 ± 0.000005 | 3.6 ± 0.13 | 2.5 ± 0.10 | 2.3 ± 0.10 | 18.1 |
| $f_2+f_3$ | 11.2738953 ± 0.0000043 | 2.6 ± 0.13 | 1.5 ± 0.10 | 1.3 ± 0.10 | 8.7 |
| $f_1-f_2$ | 0.1094061 ± 0.0000036 | 2.6 ± 0.13 | 1.5 ± 0.10 | 1.6 ± 0.10 | 4.0 |
| $2f_1+f_2$ | 17.1804423 ± 0.0000040 | 1.9 ± 0.13 | 1.5 ± 0.10 | 1.3 ± 0.10 | 10.9 |
| $2f_1+f_4$ | 17.163813 ± 0.000005 | 1.7 ± 0.13 | 1.4 ± 0.10 | 1.2 ± 0.10 | 10.1 |
| $2f_1+f_3$ | 17.1465842 ± 0.0000041 | 1.6 ± 0.13 | 1.3 ± 0.10 | 1.1 ± 0.10 | 9.4 |
| $2f_1+f_2+f_3$ | 22.800461 ± 0.000005 | 1.4 ± 0.13 | 1.0 ± 0.09 | 0.8 ± 0.10 | 8.3 |
| $2f_2$ | 11.3077534 ± 0.0000042 | 0.8 ± 0.14 | 0.8 ± 0.10 | 0.5 ± 0.10 | 4.6 |
| $f_1+f_2-f_3$ | 5.797141 ± 0.000005 | 1.0 ± 0.13 | 0.8 ± 0.10 | 0.8 ± 0.10 | 4.2 |
| $f_1+f_5$ | 13.661483 ± 0.000032 | 1.1 ± 0.13 | 0.7 ± 0.09 | 0.8 ± 0.10 | 4.5 |
| $f_1+f_3+f_4$ | 17.020548 ± 0.000005 | 0.9 ± 0.14 | 0.7 ± 0.10 | 0.7 ± 0.10 | 5.1 |
| $f_2+f_4$ | 11.291124 ± 0.000005 | 0.8 ± 0.14 | 0.7 ± 0.10 | 0.6 ± 0.10 | 4.0 |
| $f_1+f_2+f_4$ | 17.054406 ± 0.000005 | 0.8 ± 0.14 | 0.6 ± 0.10 | 0.8 ± 0.10 | 4.4 |
| $f_1-f_4$ | 0.1260358 ± 0.0000042 | 1.7 ± 0.13 | 0.6 ± 0.10 | 0.8 ± 0.10 | 1.6 |
| $f_1+2f_2$ | 17.071036 ± 0.000005 | 0.6 ± 0.14 | 0.5 ± 0.10 | 0.4 ± 0.10 | 3.6 |
| $f_3+f_4$ | 11.257266 ± 0.000005 | 0.5 ± 0.14 | 0.5 ± 0.10 | 0.3 ± 0.10 | 2.9 |

We shall now discuss the two problematic frequencies, $f_6$ and $f_{12}$, mentioned in the first paragraph of this section. In case of $f_6$, the central peak at 6.2438 $d^{-1}$ was only slightly higher than the $+1$ $y^{-1}$ alias at 6.2465 $d^{-1}$. However, the 2002-3 and 2003-4 values of $f_6$ are both much closer to the frequency of the central peak than to that of the alias peak. Moreover, in each band, the nonlinear least-squares fit converged to exactly the same solution regardless of whether the starting value of $f_6$ was the frequency of the central peak, the 2002-3 value, or the 2003-4 value. We conclude that $f_6$ given in Table 6 is unlikely to be in error by 1 $y^{-1}$.

The case of $f_{12}$ is similar, but now the $-1$ $y^{-1}$ alias at 6.2210 $d^{-1}$ is the problem. In $v$ and $y$ it is almost as high as the central peak at 6.2236 $d^{-1}$, while in $u$ it is even slightly higher. Computing power spectra from the averaged $u$, $v$ and $y$ residuals, with proper weight given to each band, did not solve the problem. In Paper III, there is also the $y^{-1}$ uncertainty: the frequency is equal to 6.22304 $d^{-1}$ for Si III 455.3 nm, but for Si III 456.8 and 457.5 nm it is close to 6.2210 $d^{-1}$. The frequency given in Table 3 of Paper I is equal to the alias frequency. More data are needed to decide whether the value given in Table 6 is the correct one.

Fig. 6 shows the power spectra of the 2002-4 data prewhitened with the 36 frequencies of Table 6. In the $u$ and $y$ spectra (bottom and top panel, respectively) the highest peaks occur at 0.3142 $d^{-1}$, but in the $v$ spectrum, at 0.2625 $d^{-1}$. The corresponding amplitudes amount to 1.9 and 1.2 mmag in $u$ and $y$, and 1.1 mmag in $v$. In neither case does the signal-to-noise ratio exceed 3.4, so that these peaks are unlikely to be intrinsic. The reader may remember that in Sect. 3.1, a peak seen at 0.314 $d^{-1}$ in the 2003-4 $u$ power spectrum was also dismissed as spurious.

The highest $S/N$ peaks in Fig. 6 have frequencies equal to 5.0139 $d^{-1}$ in $u$ ($S/N = 4.5$), 13.0152 $d^{-1}$ in $v$ ($S/N = 4.2$) and 22.9440 $d^{-1}$ in $y$ ($S/N = 4.1$). The peak at 5.0139 $d^{-1}$ can be explained in terms of colour extinction in the $u$

band (see Sect. 3.1). At 13.0152 $d^{-1}$, there are low peaks in the $u$ and $y$ spectra with $S/N$ equal to 2.9 and 2.4, respectively. No peaks at 13.0152 $d^{-1}$ can be seen in the '$\mu$ Eri $-$ $\xi$ Eri' power-spectra, so that this frequency is not due to $\xi$ Eri. Finally, the frequency of 22.9440 $d^{-1}$ is very close to the combination frequency $3f_1 + f_2$. We conclude that while the latter frequency may be intrinsic, the former is probably spurious.

### 5.2 Out-of-eclipse variation of $\mu$ Eri

Combining the 2002-3 and 2003-4 out-of-eclipse differential magnitudes '$\mu$ Eri $-$ $\xi$ Eri,' we obtained time series consisting of 5818, 5823 and 5189 data-points in $u$, $v$ and $y$, respectively.

The highest peaks in successive power-spectra of these data occurred at frequencies close to those found from the 2003-4 and 2002-3 time-series separately (see Tables 5 and 4) and at the frequency $f_6' = 0.568$ $d^{-1}$, which is new. In $u$, the frequencies appeared in the order $f_1'$, $f_2'$, $f_5'$, $f_3'$ and $f_{4a}'$, where the last frequency is the $+1$ $y^{-1}$ alias of $f_4' = 1.2056$ $d^{-1}$. The two highest peaks in the sixth-run power spectrum occurred at 2.009 and 0.997 $d^{-1}$, neither of which is likely to be intrinsic. The third peak, only slightly lower than the second one, was at $f_6'$. In $v$, the order was $f_1'$, $f_2'$, $f_4'$, $f_5'$, $f_6'$ and $f_3'$, but in the third run the peak at $f_4'$ was only slightly higher than the one at $f_{4a}'$. In $y$, the order was the same as in $v$, except that in the last run the highest peak occurred at 0.997 $d^{-1}$, while the peak at $f_3'$—although present—would be missed if it were not previously found in $u$ and $v$.

The 1 $y^{-1}$ uncertainty which affects $f_4'$ did not plague other frequencies; in all other cases the yearly aliases were significantly lower than the central peak.

The results of the analysis are given in Table 7. The numbers for $f_{4a}'$ are from nonlinear least-squares fits in which the alias frequency read off the power spectrum was used as the starting value. In these fits, the other frequencies and the corresponding amplitudes were only slightly different from those given in the table.

The $u$ to $y$ amplitude ratio in Table 7 exceeds 1.2 for all frequencies. For four frequencies the ratio is greater than 1.5, while for $f_4'$ and $f_6'$, it is equal to about 1.3. However, this dichotomy may be illusory because the (formal) standard deviation of the latter number amounts to about 0.10.

The reader may have noticed that $f_1' \approx f_B$. Since neither frequency can be due to $\xi$ Eri because the amplitudes and phases do not match (see also Sect. 4.3), this curious near-equality must be an accidental coincidence.

## 6 SUMMARY AND CLUES FOR ASTEROSEISMOLOGY

### 6.1 Independent high frequencies of $\nu$ Eri

Fig. 7 shows schematically the 11 independent high-frequency terms of $\nu$ Eri derived from the combined, 2002-4 data. Comparing this figure with Fig. 4 of Paper I one can see that two of the three high-frequency "possible further signals" of Paper I are now upgraded to the status of certainty. This has already been mentioned in Sect. 3.2 and 5.1.

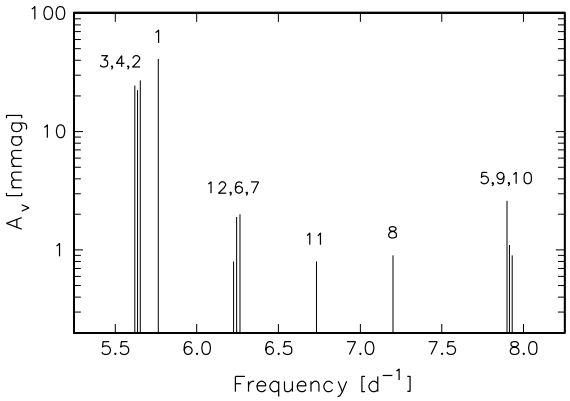


**Figure 7.** Schematic $v$-amplitude spectrum of $\nu$ Eri from the combined, 2002-4 data: the 11 independent high-frequency terms, numbered as in Table 6.

**Table 8.** The mean separation, $S$, and asymmetry, $A$, of the close frequency triplets in the oscillation spectrum of $\nu$ Eri.

| Terms | $S$ [$d^{-1}$] | $A$ [$d^{-1}$] |
|---|---|---|
| 3,4,2 | 0.0169290±0.0000022 | −0.000600±0.0000087 |
| 12,6,7 | 0.019658 ±0.000064 | −0.00118 ±0.00015 |
| 5,9,10 | 0.015860 ±0.00008 | 0.00046 ±0.00019 |

The terms in question are the $i = 9$ and 12 ones. Both are members of close frequency triplets.

The third high-frequency "possible further signal" of Paper I, with frequency equal to 7.252 $d^{-1}$, must remain in limbo. Although in the power spectra prewhitened with the 36 frequencies of Table 6 (see Fig. 6) there is a series of low peaks in the vicinity of 7.25 $d^{-1}$, the corresponding $v$-amplitudes are smaller than 0.6 mmag and the signal-to-noise ratios do not exceed 3.6. In $u$, the amplitudes are smaller than 0.8 mmag and $S/N < 3.1$. More data are needed to decide whether any of these peaks is intrinsic.

For the close frequency triplets seen in Fig. 7, the mean separation, $S$, and the asymmetry, $A$, are listed in Table 8.

In Sect. 5.1 we have warned that $f_{12}$ may be in error by 1 $y^{-1}$. If this were indeed the case, the values of $S$ and $A$ given in Table 8 for the 12,6,7 triplet should be replaced by 0.020964 and $-0.00379$ $d^{-1}$, respectively. Because of this uncertainty, and the suspicion of a long-term variation of the amplitude of the $i = 6$ term (Sect. 3.2), the triplet is not particularly suitable for asteroseismology at this stage. Fortunately, the other two triplets are well-behaved. There are no $y^{-1}$ uncertainties, even for the lowest-amplitude term of the 5,9,10 triplet, and no signs of long-term amplitude variation. In addition, the $\ell = 1$ spherical harmonic identification for all members of the large-amplitude triplet and the $i = 5$ member of the 5,9,10 one are secure (see Paper III or the Introduction). As can be seen from Fig. 8, the $i = 9$ and 10 members of the triplet have $uvy$ amplitude ratios consistent with $\ell$ equal to 1 or 2. Unfortunately, the standard deviations of the amplitude ratios, especially those of the smallest-amplitude member, are too large to fix $\ell$ unambiguously.

**Table 7.** Frequencies, periods and amplitudes in the out-of-eclipse differential magnitudes '$\mu$ Eri − $\xi$ Eri' from the combined, 2002-4 data. The last column contains the $v$-amplitude signal-to-noise ratio.

| ID | Frequency [d$^{-1}$] | Period [d] | $A_u$ [mmag] | $A_v$ [mmag] | $A_y$ [mmag] | $S/N$ |
|---|---|---|---|---|---|---|
| $f_1'$ | 0.615739 ± 0.000016 | 1.624065 ± 0.000042 | 9.9 ± 0.16 | 6.3 ± 0.12 | 5.6 ± 0.11 | 12.2 |
| $f_2'$ | 0.700842 ± 0.000034 | 1.42686 ± 0.00007 | 4.8 ± 0.16 | 3.0 ± 0.12 | 2.5 ± 0.10 | 6.5 |
| $f_4'$ | 1.205580 ± 0.000043 | 0.829476 ± 0.000030 | 3.0 ± 0.16 | 2.6 ± 0.12 | 2.4 ± 0.10 | 7.2 |
| $f_{4a}'$ * | 1.208346 ± 0.000042 | 0.827578 ± 0.000029 | 2.9 ± 0.16 | 2.5 ± 0.12 | 2.4 ± 0.10 | 6.9 |
| $f_5'$ | 0.658876 ± 0.000039 | 1.51774 ± 0.00009 | 4.0 ± 0.16 | 2.5 ± 0.12 | 2.6 ± 0.11 | 4.8 |
| $f_6'$ | 0.56797 ± 0.00005 | 1.76066 ± 0.00016 | 2.7 ± 0.16 | 2.0 ± 0.12 | 2.1 ± 0.11 | 3.1 |
| $f_3'$ | 0.81272 ± 0.00006 | 1.23044 ± 0.00009 | 2.8 ± 0.16 | 1.9 ± 0.12 | 1.4 ± 0.10 | 4.0 |

*) $f_{4a}' \approx f_4' + 1$ y$^{-1}$

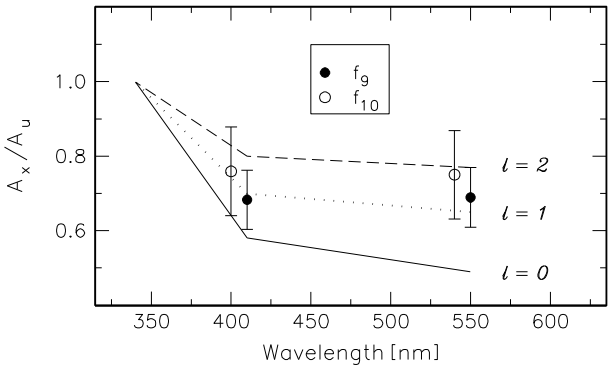


**Figure 8.** Observed $uvy$ amplitude ratios for the small-amplitude members of the 7.91 d$^{-1}$ triplet (circles with error bars) compared with theoretical amplitude ratios for $\ell \leqslant 2$. The observed ratios are from the 2002-4 amplitudes (see Table 6), the theoretical ones, from Fig. 5 of Paper III. The open circles are shifted slightly in wavelength to avoid overlap.

### 6.2 Independent low frequencies of $\nu$ Eri

As we mentioned in the Introduction, the frequency resolution of the 2002-3 data was insufficient to reject the possibility that $f_A$ is equal to the combination frequency $3f_1 - 3f_3$. As can be seen from Table 6, the difference between $f_A$ and $3f_1 - 3f_3$ amounts to 0.0030 d$^{-1}$. This number is not only much larger than the standard deviation of $f_A$, but also larger than the frequency resolution of the 2002-4 data by a factor of about 1.5. In fact, $3f_1 - 3f_3$ coincides with the $-1$ y$^{-1}$ alias of $f_A$. Since the alias has about the same height as the $+1$ y$^{-1}$ one, the combination frequency's amplitude must be below the detection threshold. Consequently, there is no longer any doubt that $f_A$ is an independent low frequency in the variation of $\nu$ Eri. In addition, we have found another low frequency, $f_B$ (see Tables 2 and 6). Since only high-order $g$ modes have frequencies that low, the suggestion put forward in Paper I that $\nu$ Eri were both a $\beta$ Cep variable and an SPB star is amply confirmed.

### 6.3 $\mu$ Eri

To the single frequency $f_1' = 0.616$ d$^{-1}$, derived from the differential magnitudes '$\mu$ Eri − $\xi$ Eri' in Paper I, we add five further ones (see Table 7). The values of the frequencies and the decrease of the $uvy$ amplitudes with increasing wavelength (for at least four frequencies) indicate that we are seeing high-radial-order $g$ modes. Thus, as already suggested in Paper I, the star is an SPB variable. Note that rotational modulation, the second hypothesis put forward in Paper I for explaining the $f_1'$ term is now untenable because it does not account for multiperiodicity.

As can be seen from Table 7, the periods $P_3'$, $P_2'$ and $P_1'$ are equally spaced, with the spacing equal to $\sim$0.20 d, while $P_4'$ precedes $P_3'$ by twice this value. The equal spacing in period may be a manifestation of the well-known asymptotic property of high-order $g$ modes of the same $\ell$. There are, however, the following two problems with this idea: (1) the term half-way between the $P_3'$ and $P_4'$ ones is missing, and (2) the period-spacing is rather large. Better data may solve the first problem if the missing term is simply too weak to be detected in our data. The second problem requires a comparison with the theory. Unfortunately, the only SPB-star model available in the literature (Dziembowski, Moskalik & Pamyatnykh 1993) has $M = 4$ M$_\odot$, $\log L/\mathrm{L}_\odot = 2.51$ and $X_c = 0.37$, whereas $\mu$ Eri is more massive (by $\sim 2$ M$_\odot$), more luminous (by $\sim$0.8 dex), and more evolved (see Paper I). In the model, the largest period spacing (for $\ell = 1$) is equal to $\sim$0.07 d, almost a factor 3 smaller than observed in $\mu$ Eri. Whether this disagreement can be alleviated with a model which better matches the star remains to be verified. If this turns out to be unsuccessful, one can still invoke the unlikely idea that an unknown amplitude limitation mechanism is suppressing the modes halfway between the observed ones.

The possibility that instead of an equally-spaced period triplet, $P_3'$, $P_2'$, $P_1'$, we have a rotationally-split frequency triplet, $f_1'$, $f_2'$, $f_3'$, is much less likely. Indeed, for an $\ell = 1$ $g$-mode with frequency equal to 0.7 d$^{-1}$ in the SPB-star model of Dziembowski et al. (1993), the observed mean separation of the frequency triplet, equal to 0.09849±0.00003 d$^{-1}$, leads to equatorial velocity of rotation, $v_e$, of about 30 km s$^{-1}$ (see their Fig. 13), whereas available estimates of $v_e \sin i$ of $\mu$ Eri range from 150 to 190 km s$^{-1}$ (see Paper I). Increasing the model's radius in order to better match $\mu$ Eri may increase $v_e$ to about 60 km s$^{-1}$, still much less than the observed values. An additional problem is posed by the large asymmetry of the frequency triplet. The asymmetry is equal to 0.0268 ± 0.0001 d$^{-1}$, while the rotational splitting seen in Fig. 13 of Dziembowski et al. (1993) is nearly symmetric.

In addition to confirming the SPB classification of Paper I, we have found $\mu$ Eri to be an eclipsing variable. As can

be seen from Figs. 3 and 5, the eclipse is a transit, probably total, the secondary is fainter than the primary by several magnitudes, and the system is widely detached. As far as we are aware, the only other eclipsing variable with similar properties is 16 (EN) Lac (Jerzykiewicz 1979), except that in the latter case the eclipse is partial. (Interestingly, the discovery of an eclipse of this well-known $\beta$ Cephei variable was a by-product a three-site campaign undertaken for observing the star's pulsations.) Solving the $\mu$ Eri system will yield the primary's mean density and its surface gravity. This, however, is beyond the scope of the present paper.

### 6.4 $\xi$ Eri

The frequencies $f_{\rm x} = 10.8742$ and $f_{\rm y} = 17.2524$ d$^{-1}$ (see Tables 2 and 6) and the MK type of A2 V (see the Introduction) leave no doubt that the star is a $\delta$ Scuti variable. The Strömgren indices, $c_1 = 1.076$ and $b-y = 0.038$ (Hauck & Mermilliod 1998), are not reddened. This is not inconsistent with the star's Hipparcos parallax of $15.66 \pm 0.80$ mas. Using the parallax and the $V$ magnitude from Hauck & Mermilliod (1998) one gets $M_{\rm V} = 1.12 \pm 0.11$, a value which, together with the $b-y$ index, places the star about 0.02 mag to the blue of the observational blue edge of the $\delta$ Scuti instability strip in the $M_{\rm V}$ vs. $b-y$ diagram (see, e.g., Handler 2002). Apart from indicating the need for a slight revision of the blue edge, this position in the diagram suggests marginal pulsation driving as a possible explanation for the small $uvy$ amplitudes. However, in view of the star's high $v \sin i$ of 165 km s$^{-1}$ (Abt & Morrell 1995), another explanation may be provided by the hypothesis of Breger (1982) that fast rotation is a factor in limiting pulsation amplitudes.

Unfortunately, with only two small-amplitude modes the asteroseismic potential of $\xi$ Eri is insignificant.

## ACKNOWLEDGMENTS

MJ and AP's participation in the campaign was supported by KBN grant 5P03D01420. MJ would also like to acknowledge a generous allotment of telescope time and the hospitality of Lowell Observatory. GH's work was supported by the Austrian Fonds zur Förderung der wissenschaftlichen Forschung under grant R12-N02. ER thanks for the support by the Junta de Andalucia and the Direccion General de Investigacion (DGI) under project AYA2003-04651. The referee, Dr C. Simon Jeffery, helped us to improve the paper.

## REFERENCES

Abt H.A., Morrell N.I., 1995, ApJS, 99, 135
Aerts C., Waelkens C., de Pauw M., 1994, A&A, 286, 136
Aerts C. et al., 2004, MNRAS, 347, 463 (Paper II)
Ausseloos M., Scuflaire R., Thoul A., Aerts C., 2004, MNRAS, 355, 352
Breger M., 1982, PASP, 94, 845
Crow E.L., Davis F.A., Maxfield M.A., 1960, Statistics Manual. Dover Publications, New York
Cugier H., Dziembowski W.A., Pamyatnykh A.A., 1994, A&A, 291, 143
De Ridder et al., 2004, MNRAS, 351, 324 (Paper III)
Dziembowski W.A., Jerzykiewicz M., 2003, in Balona L.A., Henrichs H.F., Medupe R., eds, ASP Conf. Ser. Vol. 305, Magnetic Fields in O, B and A Stars: Origin and Connection to Pulsation, Rotation and Mass Loss. Astron. Soc. Pac., San Francisco, p. 319
Dziembowski W.A., Moskalik P., Pamyatnykh A.A., 1993, MNRAS, 265, 588
Handler G., 2002, in Sterken C., Kurtz D.W., eds, ASP Conf. Ser. Vol. 256, Observational Aspects of Pulsating B and A Stars. Astron. Soc. Pac., San Francisco, p. 113
Handler G. et al., 2000, MNRAS, 318, 511
Handler G. et al., 2004, MNRAS, 347, 454 (Paper I)
Handler G., Jerzykiewicz M., Pigulski A., Pamyatnykh A.A., 2005, in preparation
Hauck B., Mermilliod M., 1998, A&AS, 129, 431
Heynderickx D., Waelkens C., Smeyers P., 1994, A&AS, 105, 447
Hill G., 1969, Publ. DAO Victoria, 13, 323
Jerzykiewicz M., 1978, Acta astr., 28, 465
Jerzykiewicz M., 1979, IBVS No. 1552
Montgomery M.H., O'Donoghue D., 1999, Delta Scuti Star Newsletter, 13, 28
Pamyatnykh A.A, Handler G., Dziembowski W.A., 2004, MNRAS, 350, 1022
Saito K., 1976, in Fitch W.S., ed, Proc. IAU Coll. 29, Multiple Periodic Variable Stars. Akadémiai Kiadó, Budapest, 2, 47
Schwarzenberg-Czerny A., 1991, MNRAS, 253, 198

This paper has been typeset from a TEX/ LATEX file prepared by the author.